Generation of laser speckle with an integrating sphere

Glenn D. Boreman, MEMBER SPIE
Yuankun Sun*
Anthony B. James
University of Central Florida
Electrical Engineering Department
Center for Research in Electro-Optics and Lasers
Orlando, Florida 32816

Abstract. A new method for generation of laser speckle, by using an integrating sphere, is investigated. This method is of particular interest in the production of speckle patterns for modulation transfer function testing of detector arrays and would be well suited in wavelength ranges for which a transmissive diffuser is not optimum. Attributes of the speckle field investigated in this paper include the degree of polarization and first- and second-order statistics. The speckle patterns generated by the integrating sphere method are seen to closely obey the theory for statistics of speckle generated by usual means.

Subject terms: laser speckle; modulation transfer function testing.

Optical Engineering 29(4), 339-342 (April 1990).

CONTENTS

1. INTRODUCTION

This paper investigates the generation of laser speckle patterns using an integrating sphere. The multiple diffuse reflections of the laser radiation inside the sphere produce a field at the exit aperture of the sphere that is of random phase and very uniform in brightness, independent of the transverse mode profile of the laser. A speckle pattern is seen downstream from the integrating sphere. We present polarization and statistical characteristics of this speckle pattern.

The motivation for this work is the use of laser speckle patterns for modulation transfer function (MTF) testing of detector arrays.[1] Generation of the speckle pattern may be accomplished by the use of a transmissive diffuser, such as a ground glass. However, the use of transmissive diffusers in the infrared portion of the spectrum is often inconvenient for MTF testing applications because the crystalline nature of the materials involved introduces anomalies into the spatial frequency power spectrum of the speckle pattern.[2]

*Permanent address: Tianjin University, Precision Instrumentation Department, Tianjin, China.

Paper 2719 received April 19, 1989; revised manuscript received Jan. 12, 1990; accepted for publication Jan. 29, 1990.

We have chosen to investigate the integrating sphere speckle generation method in the visible portion of the spectrum to facilitate detection and data acquisition tasks. This method should be directly applicable to speckle generation in the IR, with the substitution of diffuse gold[3] as the reflector material on the interior surface of the integrating sphere.

2. EXPERIMENTAL SETUP

The experimental setup used is shown in Fig. 1(a). The laser used was a 15 mW HeNe ($\lambda = 0.6328$ µm), plane polarized. The integrating sphere was coated on its interior walls with a diffusely reflecting barium sulfate paint for use at visible wavelengths. A circular baffle inside the sphere and coated with the same material as the sphere walls blocked the direct (nonscattered) transmission of laser radiation. The integrating sphere was 25.4 mm diameter, with input and output ports of 3 mm diameter. Thus, 0.7% of the surface area of the sphere is devoted to input and output ports. In general, for a given dimension of input and output ports a larger integrating sphere will produce a better uniformity of radiance across the output aperture. However, simply from conservation of flux considerations,[4] a larger integrating sphere will produce a smaller radiance at the output aperture for a given power in the input beam. The radiance at the output port is directly proportional to the flux received at the detector array. The dimensions chosen for the sphere and the ports were thus a trade-off between flux available for the test and the radiance uniformity across the output aperture.

Since there appears to be no analytical treatment of the uniformity question available in the literature, the uniformity of the radiance at the output port was measured by directly imaging the port onto the detector array (lens focal length 25 mm, f/1.4, object distance 35 mm. A profile of image irradiance versus position is shown in Fig. 1(b). Not surprisingly, the finite aperture of the image-forming optics produces speckle effects. Even with these effects in the data, the RMS uniformity seen across the output port was calculated to be in excess of 96%,

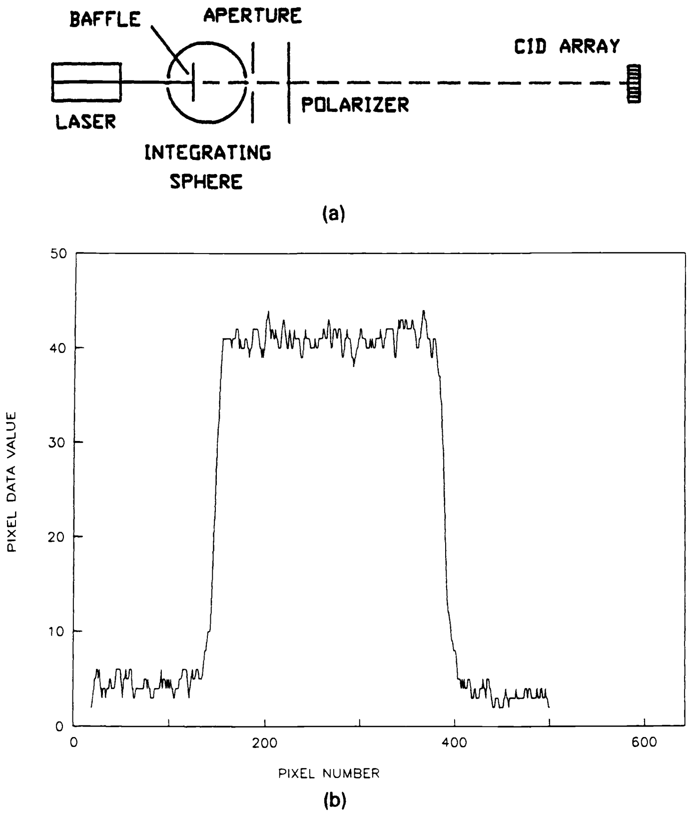

Fig. 1. (a) Experimental setup used for the production of speckle patterns. (b) Profile of irradiance vs position for an image of the output aperture of the integrating sphere.

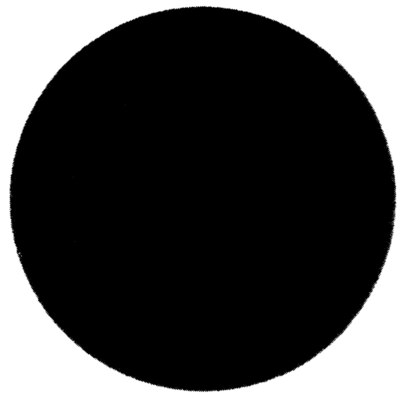

Fig. 2. Photograph of typical speckle pattern obtained. Note the shadow due to the baffle in the integrating sphere.

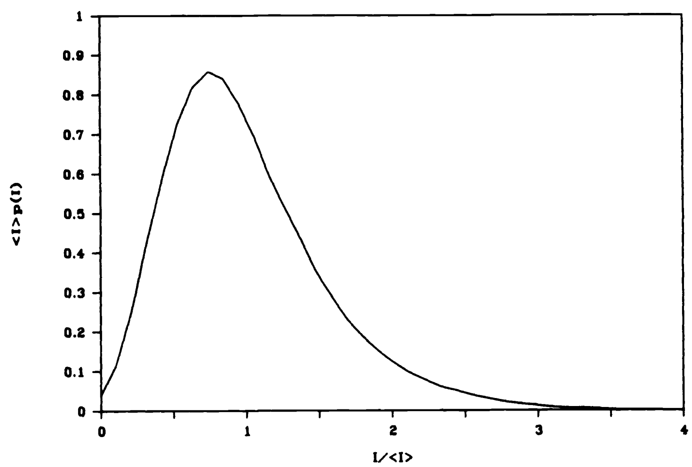

Fig. 3. Normalized speckle PDF measured inside the shadow region.

with no perceptible shading seen across the port. Without the effect of the noise due to speckle that arose in the imaging process, the actual radiance at the aperture plane would be still more uniform, in the range of approximately 98%.

A square aperture of horizontal and vertical dimensions $L = 1$ mm was placed directly at the output port of the sphere during measurement of the first- and second-order statistics. A polarizer was placed immediately after the aperture to ensure a polarized speckle pattern.

The distance z from the aperture to the receiver (detector array or photographic film) was 7.3 cm for the statistics measurements. The charge injection device (CID) detector array had horizontal rows of 376 elements, on a center-to-center spacing of 23.3 μm. The photosites were contiguous, so the effective dimension of each individual detector in the array was also 23.3 μm in the horizontal direction.

The upper limit of the spatial frequency content in the speckle pattern, ξ_{cutoff}, is given by[5] $L/\lambda z$. If the detector element spacing is Δx, then $1/2\Delta x$ is the spatial Nyquist frequency, in this case approximately 21.5 cycles/mm. The distance z was chosen so that ξ_{cutoff} was equal to the Nyquist frequency to avoid aliasing.

3. RESULTS

3.1. Degree of polarization

The degree of polarization was investigated in the following manner: The laser beam was initially plane polarized going into the integrating sphere, and the polarizer at the output of the sphere was rotated in angle to analyze the degree of polarization of the speckle. A single-element detector was placed as close as possible following the polarizer. It was found that the light exiting the integrating sphere was completely depolarized, with no dependence of received flux on the orientation of the analyzer.

3.2. First-order statistics

A qualitative investigation of the first-order statistics of the speckle irradiance yields the pattern seen in the photograph in Fig. 2. A shadow of the baffle in the integrating sphere may be clearly seen. This shadow effect is quite pronounced since the 1 mm × 1 mm aperture used at the output port produces a pinhole camera imaging situation. The scale of this pattern was such that the entire detector array could be placed either in the shadow region or in the bright region. This was the setup used for measurement of the first- and second-order statistics for the detected speckle irradiance in each region.

The data processing procedure used for calculation of the probability density function (PDF) for each region was as follows: With the CID array located inside the shadow or outside the shadow, a frame of speckle data was taken from the camera's video output. In both cases, a subtraction of the dark current

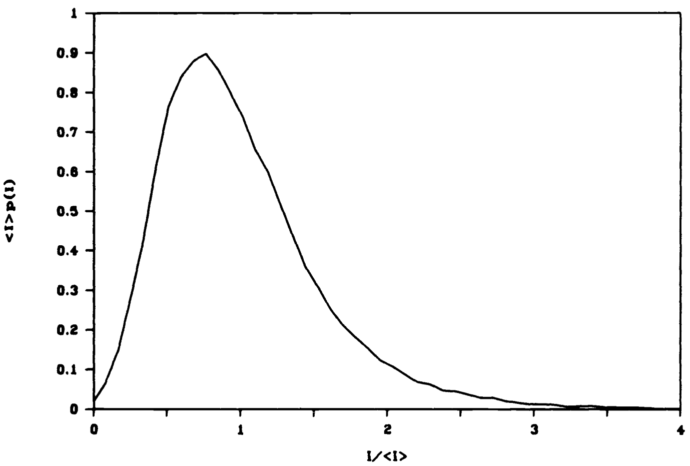

Fig. 4. Normalized speckle PDF measured outside the shadow region.

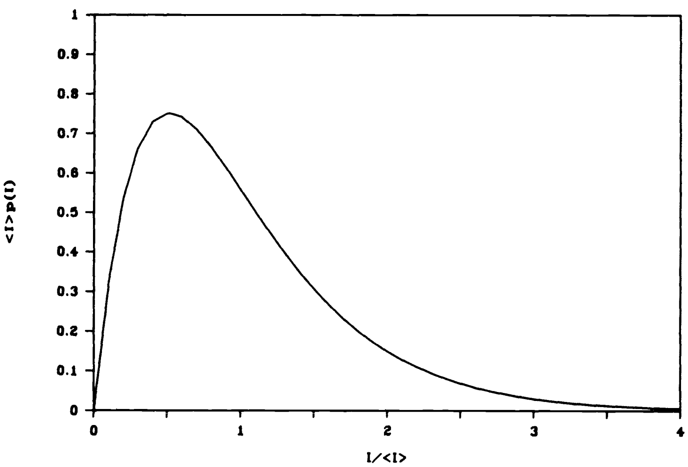

Fig. 5. Normalized speckle PDF calculated from Eqs. (1) and (2).

background was made. A histogram of signal levels was then performed on a 256×256 window of the data.

From this data, a calculation of the mean irradiance in each region yielded a 45% higher value in the bright region as compared to the shadow region. To compare the measured PDFs to theoretical curves, they have been plotted in a normalized form as $\langle I\rangle p(I)$ versus $I/\langle I\rangle$, where $\langle I\rangle$ is the mean irradiance for that region. Figures 3 and 4 show the resulting normalized PDFs inside and outside the shadow. The two curves are of approximately identical shape. This shape is characteristic of speckle that has been received over a finite size detector aperture.[6–8] The approximate method of Ref. 6 was used to calculate the theoretical PDF seen in Fig. 5. The analytical form is

$$\langle I\rangle p(I) = \frac{\mathcal{M}^{\mathcal{M}}\left(\frac{I}{\langle I\rangle}\right)^{\mathcal{M}-1}\exp[-\mathcal{M}(I/\langle I\rangle)]}{\Gamma(\mathcal{M})} . \quad (1)$$

$\mathcal{M}$ is a correlation parameter, which may be calculated as follows from the measurement aperture area S_m and the speckle correlation area S_c: For a square aperture at the original scattering plane,

$$\mathcal{M} = \frac{2}{\sqrt{S_m}}\int_0^\infty\left(1-\frac{x}{\sqrt{S_m}}\right)\mathrm{sinc}^2\left(\frac{x}{\sqrt{S_c}}\right)dx , \quad (2)$$

which yielded a value of $\mathcal{M} = 2.043$ for our measurement conditions. Comparison of Fig. 5 with Figs. 3 and 4 yields a reasonable agreement as to the shape of the normalized PDF curves. Indeed, the more exact analytical methods of Refs. 7 and 8 seem to indicate a variation of this sort.

3.3. Second-order statistics

The second-order statistics of the speckle irradiance, the spatial frequency power spectral density (PSD), was calculated in the following manner: For a given digitized frame of speckle data $d(x,y)$ with the background subtracted, a 1-D PSD estimate was made for each of 256 rows of data. These 256 PSD estimates were then ensemble averaged to obtain a better signal-to-noise ratio in the PSD.[9]

$$\mathrm{PSD}(\xi) = \langle|\mathcal{F}_x\{d(x,y)\}|^2\rangle , \quad (3)$$

where the brackets denote the ensemble averaging operation performed over the rows (y direction), $\mathcal{F}_x$ denotes a 1-D Fourier transform along x, and ξ denotes the spatial frequency variable in the x direction.

For polarized speckle, the PSD of the laser speckle irradiance (at the input to the detector array) is proportional to a scaled version of the autocorrelation of the aperture function (Ref. 5). For the uniformly illuminated square aperture used, the input PSD is thus of triangular shape, with a cutoff frequency of $\xi_{\mathrm{cutoff}} = L/\lambda z$. As discussed in Sec. 2, this cutoff frequency was chosen to be the spatial Nyquist frequency of the array (21.5 cycles/mm), to avoid aliasing.

The output PSD of the speckle (after detection) has been filtered (multiplied) by the MTF of the detector array, which allows the detector array MTF to be calculated (Ref. 1) from the output PSD as

$$\mathrm{MTF}(\xi) = \frac{\mathrm{PSD}_{\mathrm{output}}(\xi)}{\mathrm{PSD}_{\mathrm{input}}(\xi)} . \quad (4)$$

The ensemble-averaged PSDs are shown as Fig. 6 (inside the shadow region) and Fig. 7 (outside the shadow region). While both PSDs have approximately the same shape and cutoff frequency, the PSD resulting from the region of lower irradiance does exhibit a somewhat lower signal-to-noise ratio.

The PSD data from Fig. 7 were fit with a second-degree polynomial. This allows the calculation of detector array MTF by Eq. (4). Figure 8 shows three curves. The upper curve is the calculated MTF of the detector array. The middle curve is the input power spectrum $\mathrm{PSD}_{\mathrm{input}}(\xi)$, and the bottom curve is the polynomial fit to the output power spectrum $\mathrm{PSD}_{\mathrm{output}}$ from Fig. 7.

The calculated MTF can be seen to increase near the spatial Nyquist frequency. This artifact results from the denominator in Eq. (4) approaching the baseline noise of the system, yielding an approximately constant output, while the input PSD is still decreasing, as a function of spatial frequency.

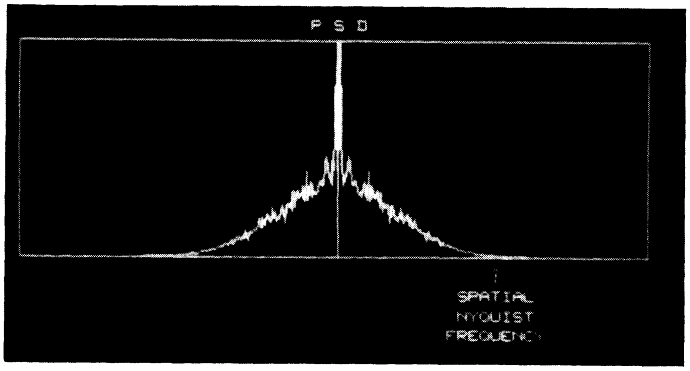

Fig. 6. PSD measured for speckle inside the shadow region. The arrow indicates the spatial Nyquist frequency of 21.5 cycles/mm.

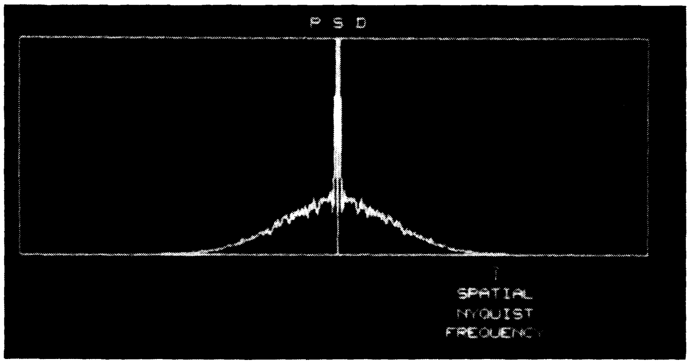

Fig. 7. PSD measured for speckle outside the shadow region. The arrow indicates the spatial Nyquist frequency of 21.5 cycles/mm.

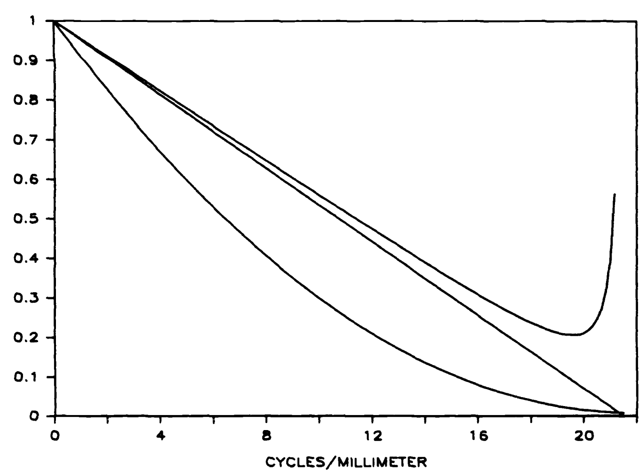

Fig. 8. Upper curve is the calculated MTF of the detector array. The middle curve is the input PSD of the speckle. The bottom curve is the polynomial fit to the normalized output PSD of the speckle from Fig. 7.

4. CONCLUSIONS

A new method of generating laser speckle using an integrating sphere has been shown to produce speckle with first- and second-order statistics that closely obey the usual theories. This method should be of use in the production of calibratable speckle patterns for testing of optical systems in wavelength regions where the use of transmissive diffusers is inconvenient due to materials considerations.

5. ACKNOWLEDGMENTS

This work was supported by a University of Central Florida In-House Research Grant and by the Florida High Technology and Industry Council. Thanks are also due to J. T. Lin of UCF for providing the support of Y. Sun during this project.

6. REFERENCES

1. G. D. Boreman and E. L. Dereniak, "Method for measuring MTF of charge coupled devices using laser speckle," Opt. Eng. 25(1), 148–150 (1986).
2. G. D. Boreman, "Measurement of MTF of a HgCdTe focal plane array using laser speckle at 9.5 microns," Univ. of Central Florida Final Rept. to U.S. Army Night Vision Lab., Contract #DAAG29-81-D-0100 (Sept. 1986).
3. Integrating Sphere Catalog, Labsphere Co., North Sutton, N.H. (1987).
4. K. F. Carr, "Integrating sphere flux calculations," Tech. Note #1, Labsphere Co., North Sutton, N.H. (1988).
5. J. Goodman, in *Laser Speckle and Related Phenomena,* J. C. Dainty, ed., p. 39, Springer-Verlag, Berlin (1975).
6. J. Goodman, in *Laser Speckle and Related Phenomena,* J. C. Dainty, ed., pp. 46–58, Springer-Verlag, Berlin (1975).
7. R. Barakat, "First-order probability densities of laser speckle patterns observed through finite-size scanning apertures," Opt. Acta, 20(9), 729–740 (1973).
8. A. A. Scribot, "First-order probability density functions of speckle measured with a finite aperture," Opt. Commun. 11(3), 238–241 (1974).
9. J. S. Bendat and A. G. Piersol, *Random Data: Analysis and Measurement Procedures,* pp. 189–193, Wiley-Interscience, New York (1971).

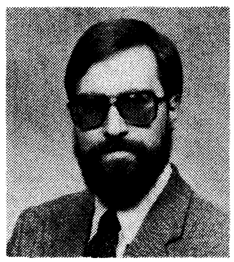

Glenn D. Boreman received the BS degree in optics from the University of Rochester in 1978 and the Ph.D. degree in optical sciences from the University of Arizona in 1984. He has held visiting technical staff positions at ITT, Texas Instruments, the U.S. Army Night Vision Laboratory, and McDonnell Douglas. Dr. Boreman has been at the University of Central Florida since 1984 and is currently an associate professor of electrical engineering. He is a member of OSA, SPIE, and SPSE and currently serves as president of the Florida Section of the OSA.

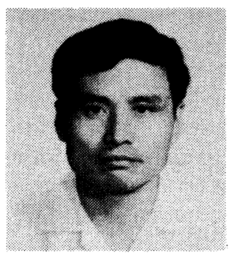

Yuankun Sun received a BS degree in applied optics in 1970 from Changchun Institute of Optics and Fine Mechanics, China, and an MS degree in optics in 1982 from Tianjin University, China. He is pursuing his Ph.D. degree in electro-optics and lasers at the University of Central Florida, working on phase conjugation and its application to optical information processing, laser speckle, and two-wave mixing. From 1970 to 1987 he was both a faculty member and a graduate student at Tianjin University, doing research working in lasers, optical holography, fiber optics, laser speckle, and optical phase conjugation.

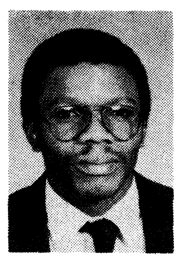

Anthony B. James received the BS degree in electrical engineering from Pratt Institute in New York in 1984 and the MS degree in electrical engineering from the University of Central Florida in 1989. He has held technical staff positions at Garland Instruments and at ACE, Inc., both in Dallas, Texas. Mr. James is a graduate research assistant at the Center for Research in Electro-Optics and Lasers at UCF. He is a member Tau Beta Pi.